Measurement report: Sources, sinks and lifetime of NO_X in a sub-urban temperate forest at night

Supplementary information

Simone T. Andersen[1], Max R. McGillen[2], Chaoyang Xue[2], Tobias Seubert[1], Patrick Dewald[1], Gunther N. T. E. Türk[1], Jan Schuladen[1], Cyrielle Denjean[3], Jean-Claude Etienne[3], Olivier Garrouste[3], Marina Jamar[4], Sergio Harb[5], Manuela Cirtog[5], Vincent Michoud[6], Mathieu Cazaunau[5], Antonin Bergé[5], Christopher Cantrell[5], Sebastien Dusanter[4], Bénédicte Picquet-Varrault[5], Alexandre Kukui[7], Abdelwahid Mellouki[2,8], Lucy J. Carpenter[9], Jos Lelieveld[1], John N. Crowley[1]

[1]Atmospheric Chemistry Department, Max-Planck-Institute for Chemistry, 55128-Mainz, Germany

[2]Institut de Combustion, Aérothermique, Réactivité Environnement (ICARE), CNRS, 1C Avenue de la Recherche Scientifique, CEDEX 2, 45071 Orléans, France

[3]CNRM, Universite de Toulouse, Meteo-France, CNRS, Toulouse, France

[4]IMT Nord Europe, Institut Mines-Télécom, Université de Lille, Center for Energy and Environment, 59000 Lille, France

[5]Univ Paris Est Creteil and Université de Paris Cité, CNRS, LISA, F-94010 Créteil, France

[6]Université Paris Cité and Univ Paris Est Creteil, CNRS, LISA, F-75013 Paris, France

[7]Laboratoire de Physique et Chimie de l'Environnement et de l'Espace (LPC2E), CNRS Orléans, France

[8]University Mohammed VI Polytechnic (UM6P), Lot 660, Hay Moulay Rachid Ben Guerir, 43150, Morocco

[9]Wolfson Atmospheric Chemistry Laboratory, Department of Chemistry, University of York, York, UK

Includes:

Figure S1-S11

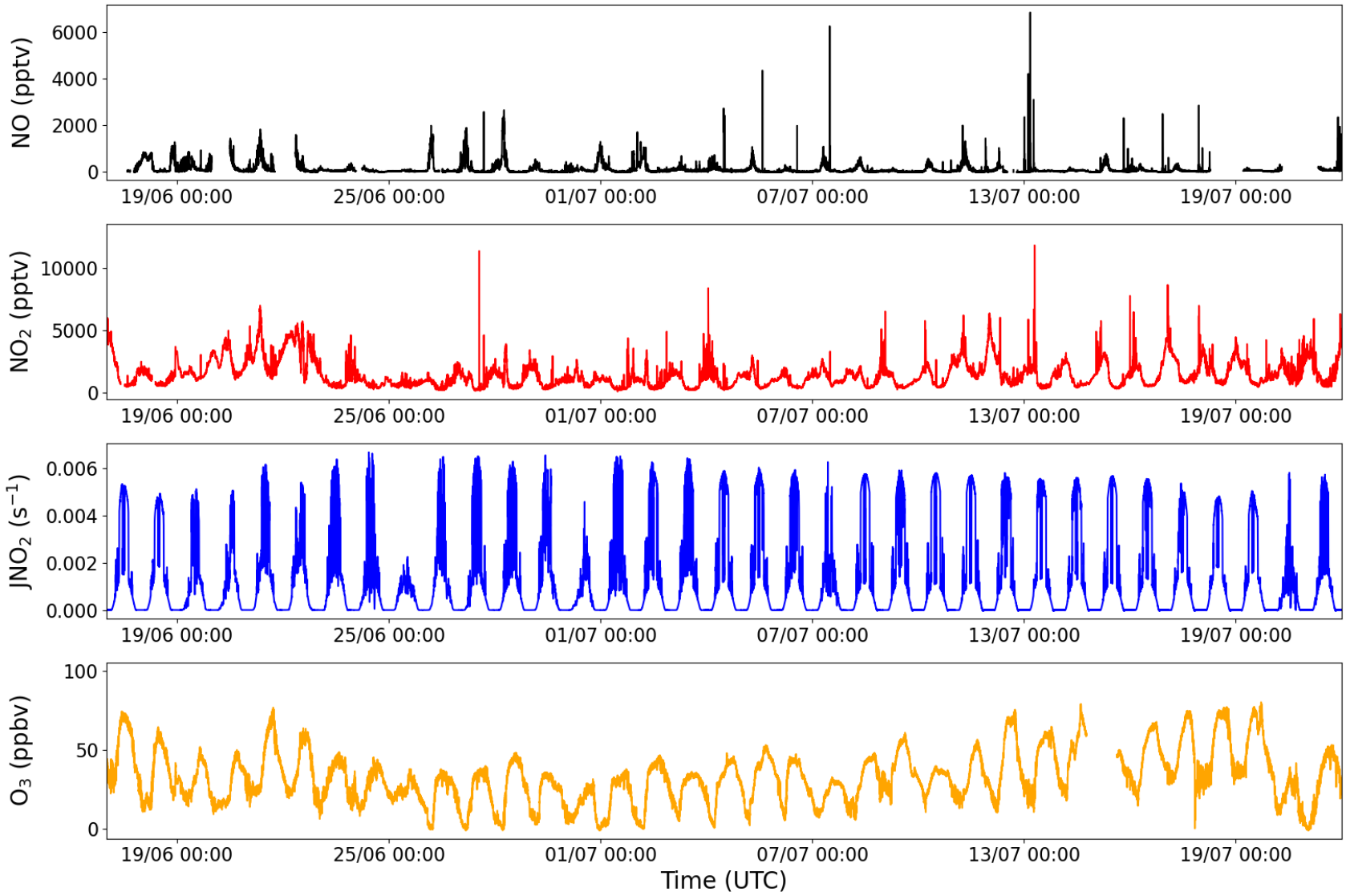

Figure S1: Time series of NO, NO_2, JNO_2, and O_3 between June 17th 2022 and July 22nd 2022 measured at 3-6 m above ground at the Rambouillet supersite during ACROSS.

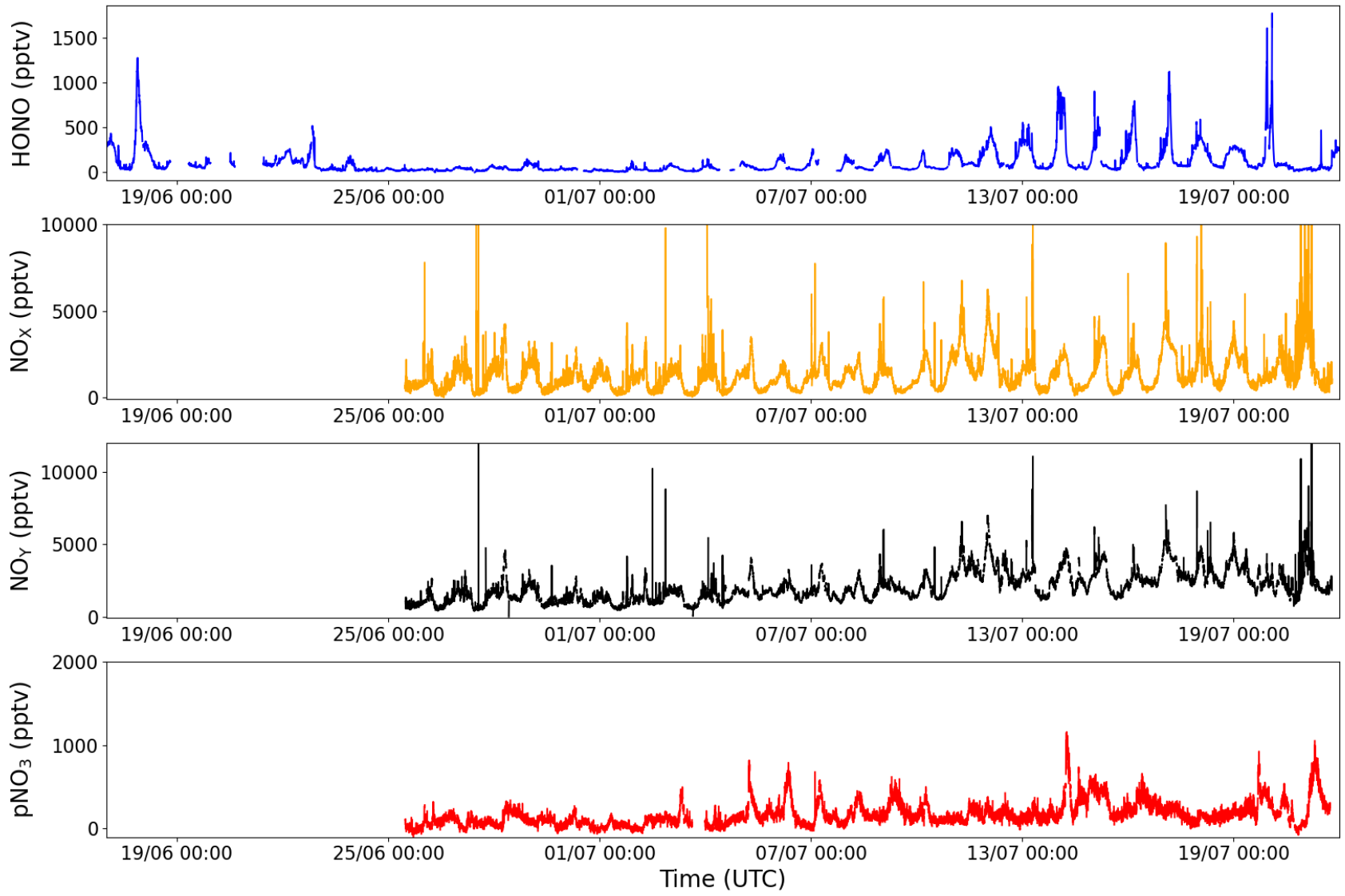

Figure S2: Time series of total NO_x, NO_y, and particulate nitrate (pNO_3) between June 17th 2022 and July 22nd 2022 measured at 2-6 m above ground at the Rambouillet supersite during ACROSS.

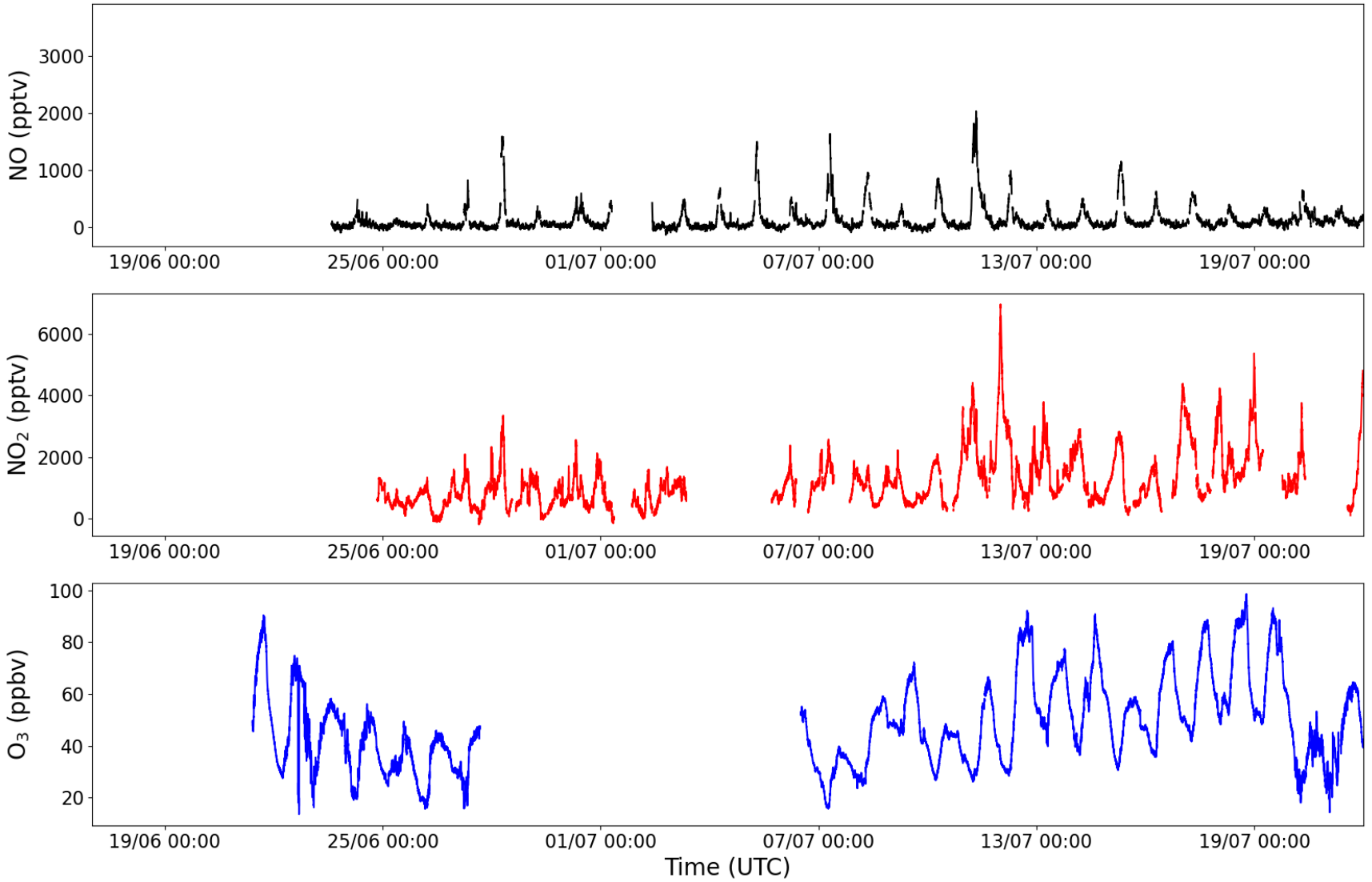

Figure S3: Time series of NO, NO_2, and O_3 between June 17th 2022 and July 22nd 2022 measured at 41 m above ground at the Rambouillet supersite during ACROSS.

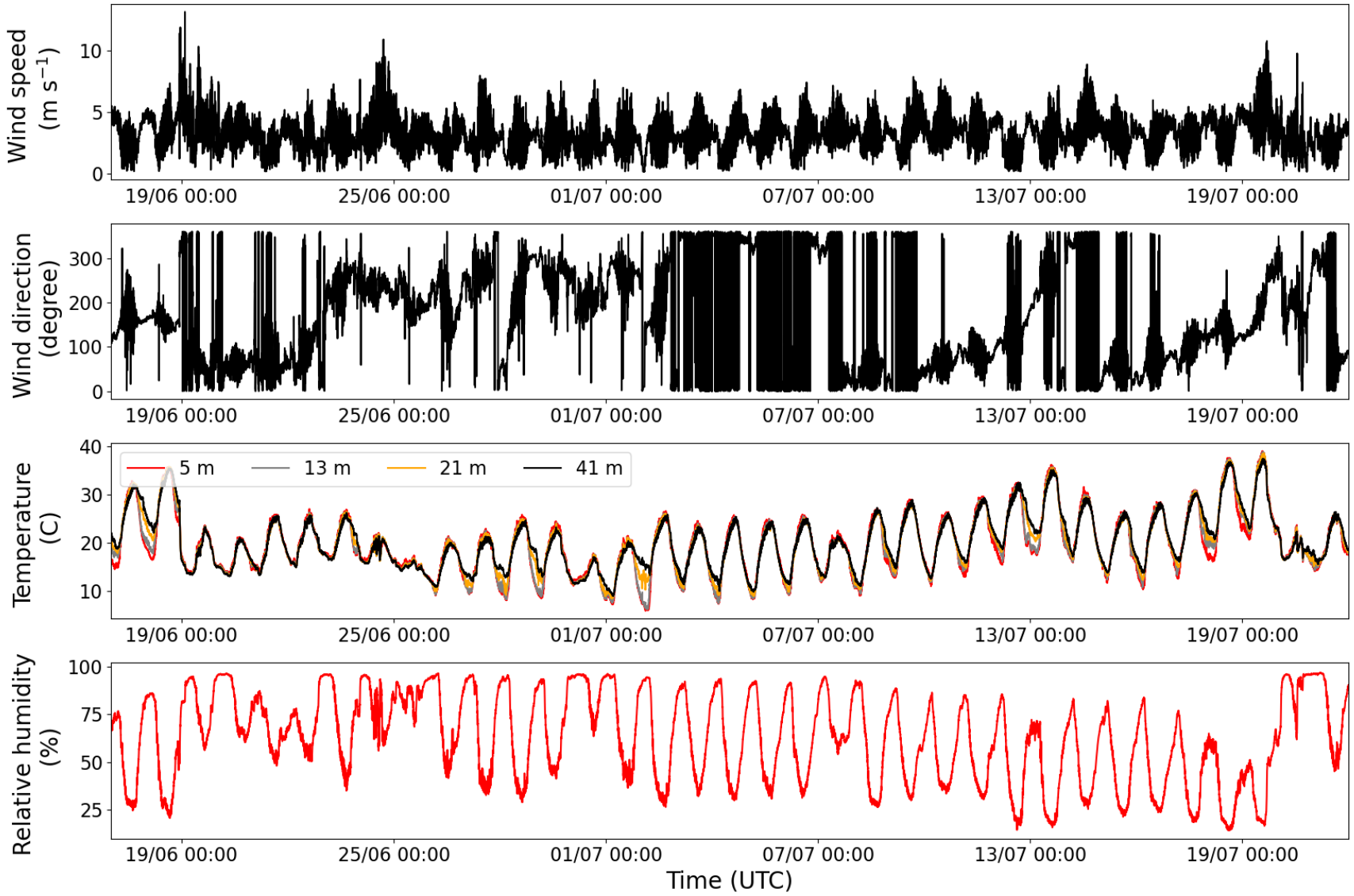

Figure S4: Time series of wind speed and direction, temperature, and relative humidity between June 17th 2022 and July 22nd 2022 measured at 5 m (red), 13 m (grey), 21 m (orange), and 41 m (black) above ground at the Rambouillet supersite during ACROSS.

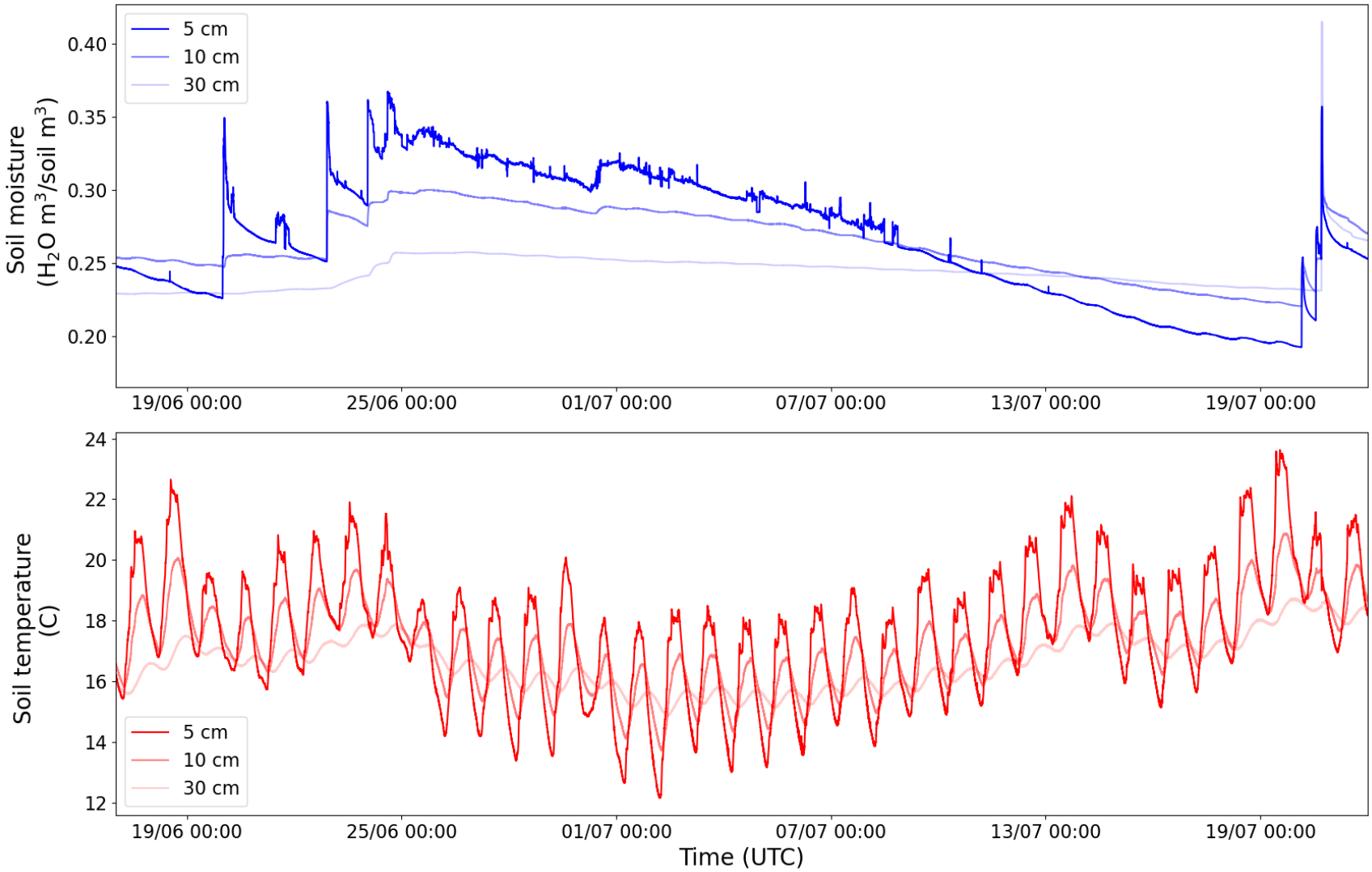

Figure S5: Time series of soil moisture and temperature between June 17th 2022 and July 22nd 2022 measured at 5, 10 and 30 cm below ground at the Rambouillet supersite during ACROSS.

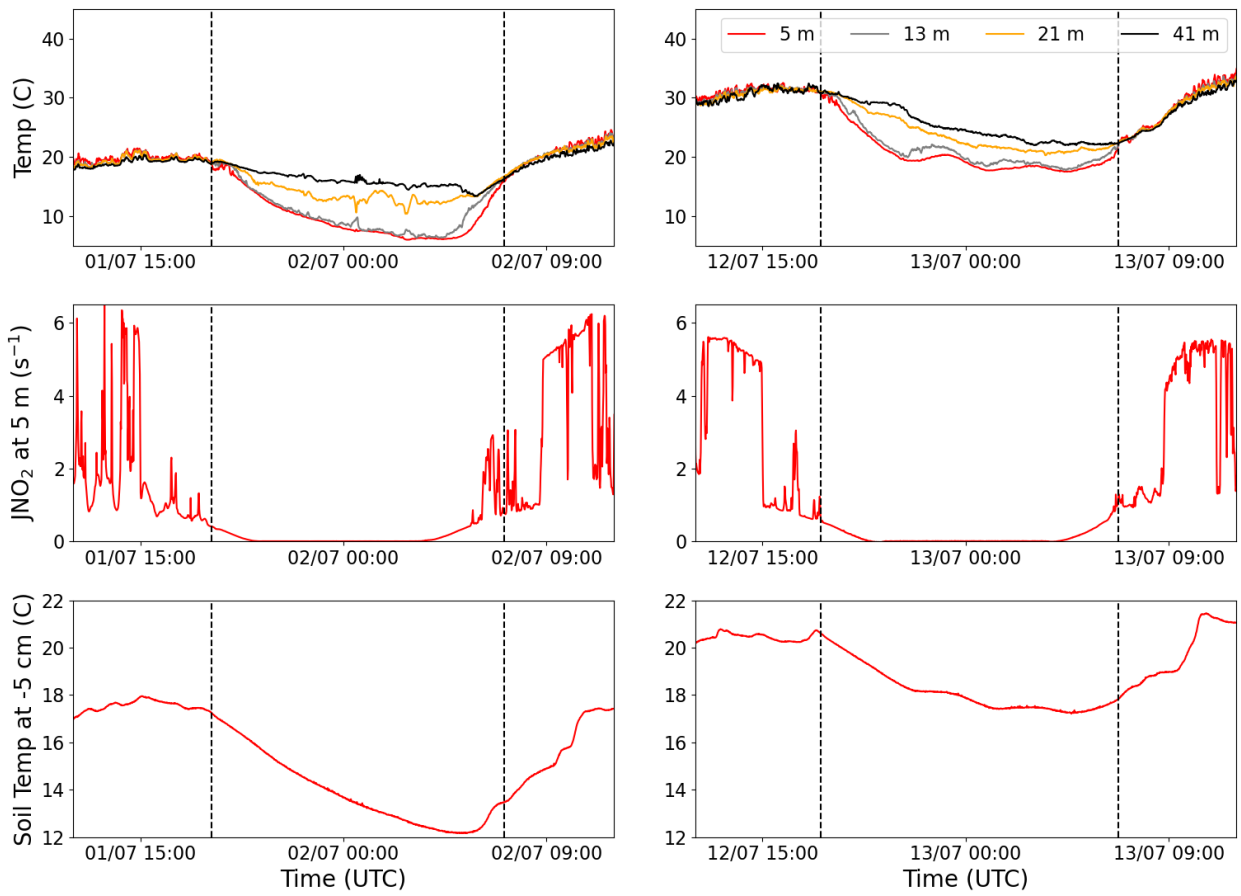

Figure S6: Temperature at 5 m (red), 13 m (grey), 21 m (orange), and 41 m (black), NO_2 photolysis rates (JNO_2) at 5 m, and soil temperature 5 cm below the surface plotted for two nights during ACROSS with large temperature inversions (beginning and end marked with dashed black lines). The temperature inversions begin on both nights when the soil temperature begins to decrease.

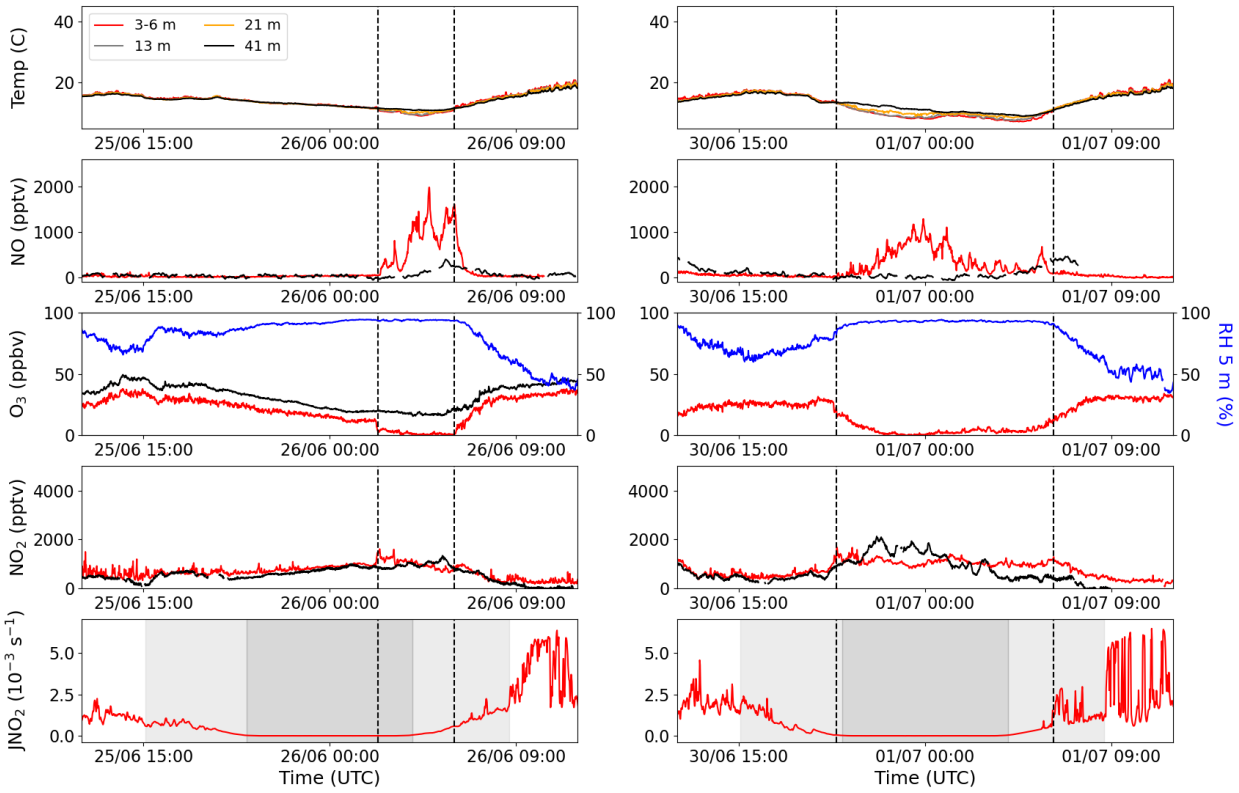

Figure S7: Measurements of temperature, NO, O_3, RH, NO_2, and JNO_2 for two different nights during the Atlantic part of the campaign. The different colours symbolize four different heights; red = 3-6 m, grey = 13 m, orange = 21 m, and black = 41 m, and the blue shows the RH at 5 m. The grey shaded areas in the JNO_2 plots shows the time the MPIC container was in shade during the afternoon and morning (light grey) and nighttime (dark grey). The vertical black dashed lines indicate the beginning and end of the observed temperature inversions in the top panels.

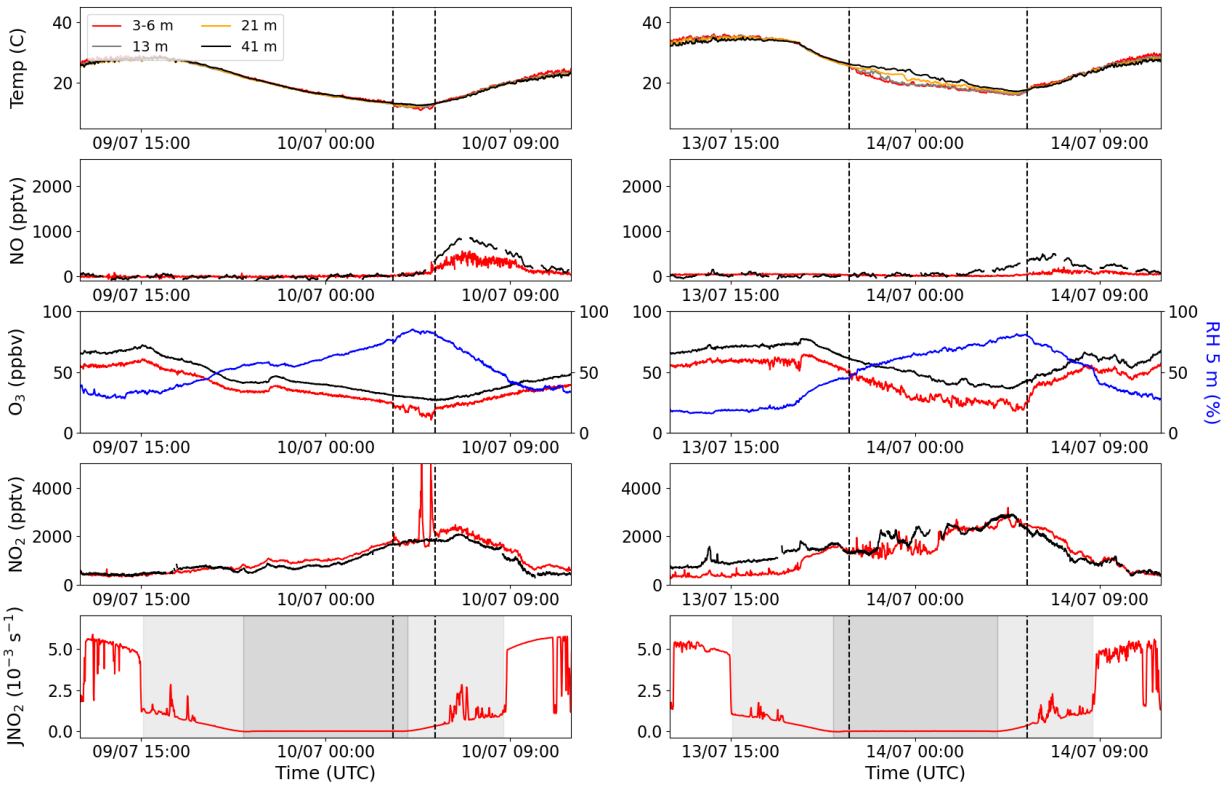

Figure S8: Measurements of temperature, NO, O_3, RH, NO_2, and JNO_2 for two different nights during the Continental part of the campaign. The different colours symbolize four different heights; red = 3-6 m, grey = 13 m, orange = 21 m, and black = 41 m, and the blue shows the RH at 5 m. The grey shaded areas in the JNO_2 plots shows the time the MPIC container was in shade during the afternoon and morning (light grey) and nighttime (dark grey). The vertical black dashed lines indicate the beginning and end of the observed temperature inversions in the top panels.

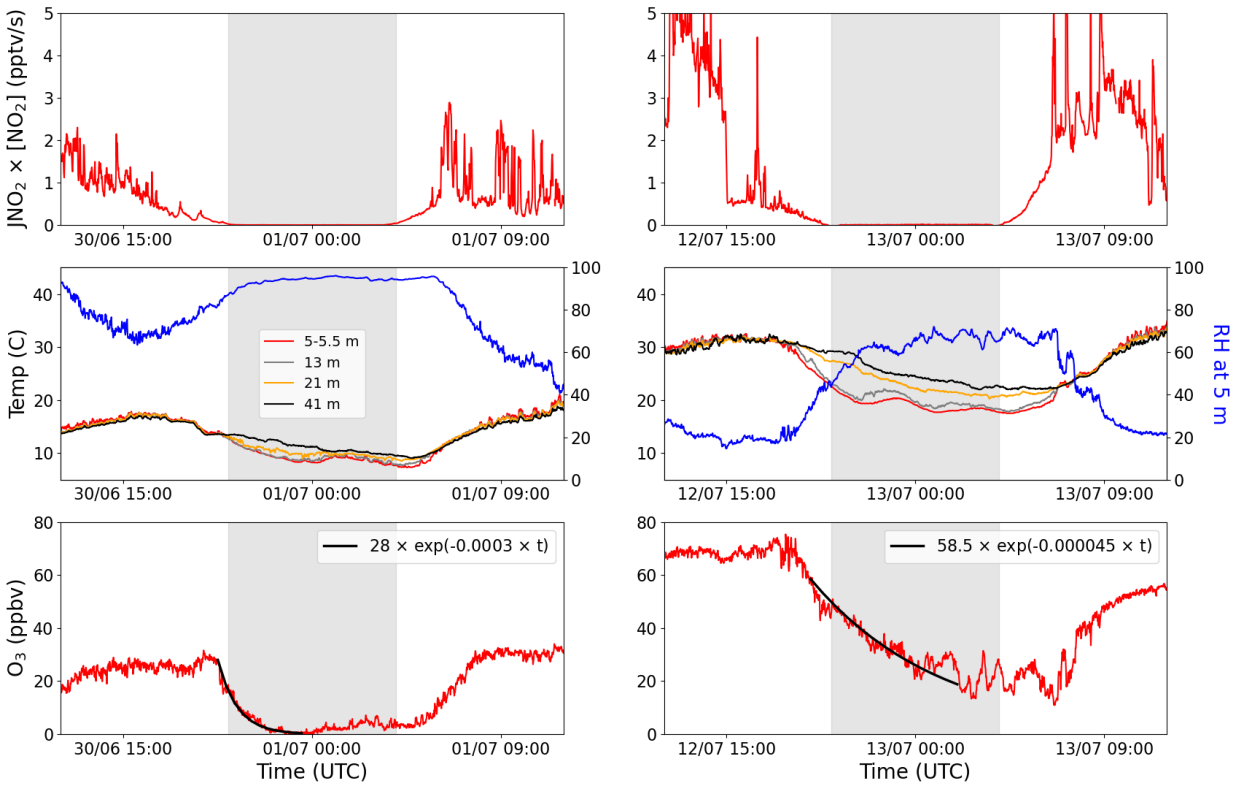

Figure S9: The production of O_3 ($JNO_2 \times [NO_2]$), temperature, RH, and O_3 plotted for two nights with observed temperature inversions; one high RH (left panels) and one with lower RH (right panels). The different colours symbolize four different heights; red = 5-5.5 m, grey = 13 m, orange = 21 m, and black = 41 m, and the blue shows the RH at 5 m. The net nighttime O_3 loss if fitted with an exponential decay curve in the bottom plots. The grey shaded areas show the nighttime, where no sunlight is present.

Corrections applied to the CLD NO-dataset

As indicated in the main text, a chemiluminescence device (CLD) was used for measurement of NO. The basic operational principal is the optical detection of fluorescence from NO_2* (electronically excited NO_2) following its formation in the reaction of NO with a large excess of O_3. The fractional conversion of NO to NO_2* and thus the sensitivity of the CLD depends on the reaction time and the concentration of O_3. O_3 is formed via O_2 photolysis using the 184.95 nm line of a low-pressure Hg-lamp. In normal operation, the amount of O_3 is maximised by using pure O_2 instead of air as the photolyte. During the ACROSS campaign the supply of O_2 was interrupted for several days (02.07.2022 at ~ 15:00 to 12.07.2022 at ~ 09:30) in which time an air flow was used instead. As calibrations of the CLD were not carried out during the campaign, the loss of sensitivity in this period was established by comparing CLD-NO measurements with those calculated from NO_X – NO_2, both measured using cavity-ring-down-spectroscopy, CRDS during the three phases (times are UTC) defined as:

Phase 1 CLD operation with O_2 (until 02.07.2022, 15:00)

Phase 2 CLD opertion with air (02.07.2022, 15:00 to 12.07.2022, 09:30)

Phase 3 CLD operation with O_2 (12.07.2022, 09:30 until end of campaign)

On order to do this as accurately as possible, we used only time periods in which features in the the CRDS-(NO_X-NO_2) were well above detection limit for prolonged periods.

Correlation plots of NO (CLD) versus NO_X-NO_2 (CRDS) are shown below for distinct NO features during each campaign phase. In each case, correction factors were applied to the NO (CLD) dataset to generate a slope of unity. The correction factors thus derived are 0.77 (Phase 1), 2.21 (Phase 2) and 0.91 (Phase 3). As expected, a large correction factor was required to allign the data in phase 2, when the CLD was operated with air instead of O_2. The ratio of CLD sensitivity to NO when using O_2 compared to air is 2.6 ± 0.2.

A correction procedure was also applied to the NO (CLD) dataset to account for differences in the back-ground signal during each of the phases described above. In order to do this, we make the assumption that the most frequent NO mixing ratio at nightime is zero, as evidenced by periods of very low variabilty (in contrast to NO_2). Apparent NO mixing ratios well above zero (up to 100 pptv) on some nights which displayed little or no variability are unlikely to be real but related to too-infrequent zeroing of the instrument, which was carried out only a few times during the campaign. The maximum in the frequency distribution of the NO mixing ratio was oberved in bins centered at 50, 10 and 110 ppt for phases 1, 2 and 3, respectively. These values were thus subtracted from the NO (CLD) measurements.

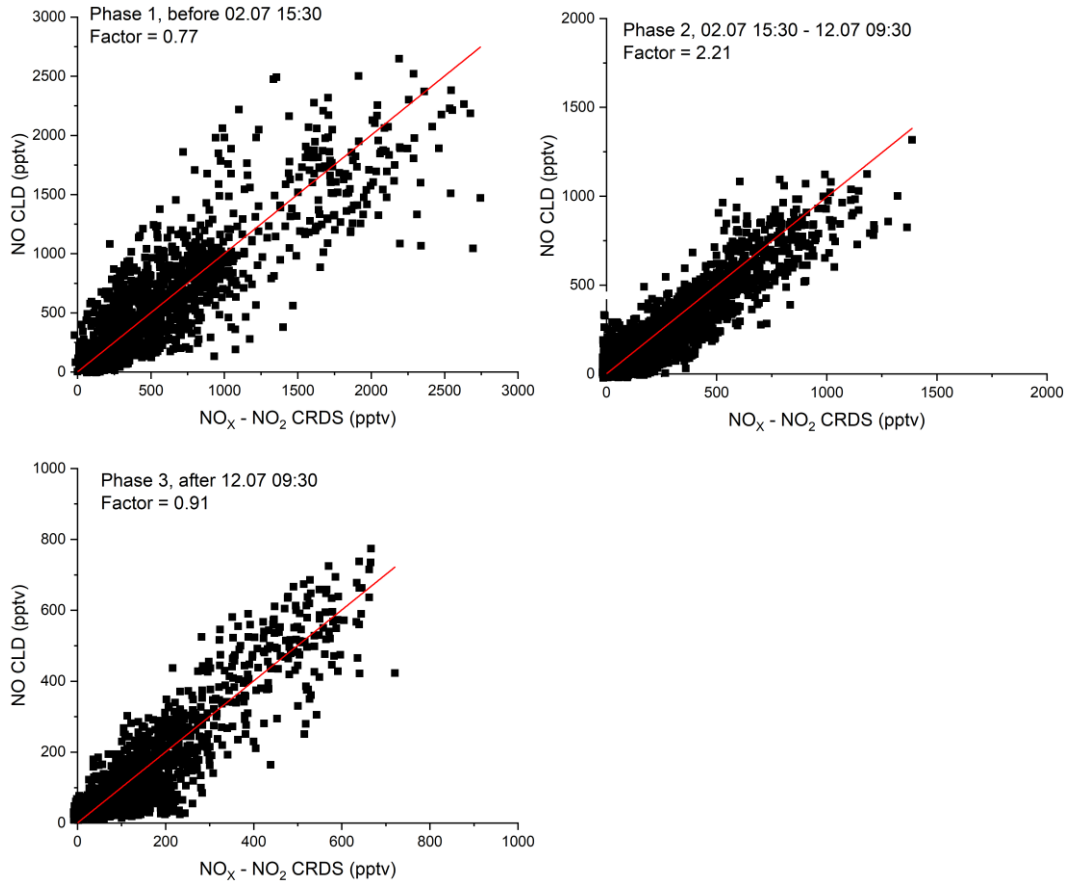

Figure S10. Plot of NO (measured by the CLD) versus NO_X – NO_2 (measured by CRDS) during three campaign phases. In each case, the factor in the legend has been applied to the NO (CLD) dataset to generate a slope of 1.

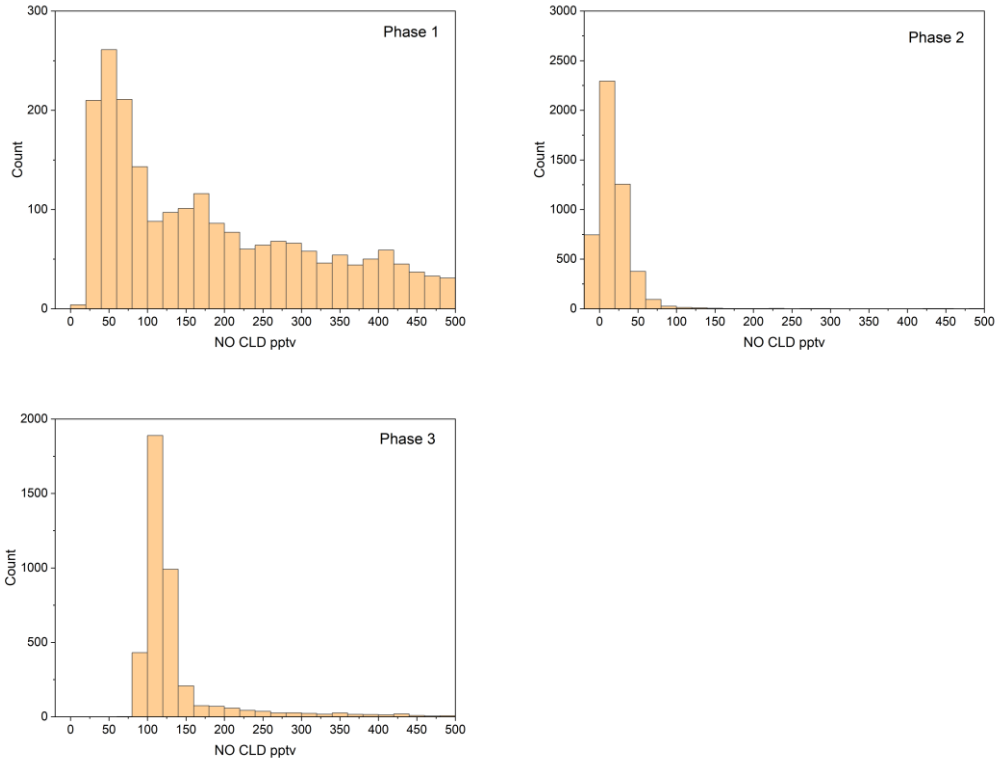

Figure S11. Frequency distribution of NO (CLD) measurements at nightime during ACROSS. The Phases are the same time periods as described above and in Fig. S10. The NO mixing-ratio in the bin centered at the peak of the distribution was subtraced from the NO-dataset.